PROCEEDINGS REPRINT

SPIE—The International Society for Optical Engineering

Reprinted from

Optical Instruments for Weather Forecasting

8–9 August 1996
Denver, Colorado

SPIE P PROCEEDINGS SERIES

Volume 2832

Lower tropospheric temperature measurement using a rotational Raman lidar

Franz Balsiger, Paul A. T. Haris*, C. Russell Philbrick

The Pennsylvania State University
Applied Research Laboratory
P.O. Box 30, State College, PA 16804
fxb9@psu.edu crp3@psu.edu

ABSTRACT

The performance of the **L**idar **A**tmospheric **P**rofile **S**ensor (LAPS) instrument for temperature measurements in the lower troposphere has been investigated. LAPS is an automated lidar system that measures temperature from the rotational Raman return of atmospheric nitrogen and oxygen. We present the measurement technique, the data analysis and the performance of the LAPS instrument. Comparisons to radiosonde profiles are discussed.

Keywords: Automated operational lidar, rotational Raman scatter, temperature measurements, troposphere

1 INTRODUCTION

Using **L**idar **A**tmospheric **M**easurment **P**rogram (LAMP) lidar instrument, our laboratory has previously investigated the possibility of using the vibrational N_2 Raman profile for temperature measurements in the regions contaminated by particle and aerosol scattering.[1] The investigation of Rau has shown that the N_2 Raman profile can be used for temperature determinations in some cases.[2] However, in the presence of layers of particles and aerosols in troposphere, its use is very limited. The necessary corrections for the extinction can only be applied when no significant cloud scattering layers are present and when simplifying assumptions about the particle scattering can be made. An elegant way to avoid these problems is to measure the ratio of two parts of the rotational Raman spectrum from N_2 and O_2. The LAMP lidar has been used during the past several years to investigate the rotational Raman temperature measurement. The rotational Raman technique for temperature measurements was first reported by Cooney in 1972.[3] A double grating monochrometer was used by Arshinov, et al.[4] to measure the rotational Raman spectrum in 1983. Hauchecorne, et al.[5] and Nedeljkovic, et al.[6] demonstrated the capability to measure the temperature using narrowband filter technology in the upper troposphere and lower stratosphere.

*Current address: Phillips Laboratory/SX, BLDG 592, 3550 Aberdeen Ave SE, Kirtland AFB NM 87117-5776

0-8194-2220-7/96/$6.00

2 INSTRUMENT

The **L**idar **A**tmospheric **P**rofile **S**ensor (LAPS) was designed as an automated system to measure water vapor and temperature in the lower troposphere in order to determine refractivity profiles.[1] The water vapor measurement is based on vibrational Raman scatter, the temperature measurement is based on rotational Raman scatter. LAPS consists of a console and a deck unit which are connected over a 23 m fiber optic cable. The laser beam diameter is expanded by a factor of five and sent into the sky coaxial to the receiving telescope. The prime focus parabolic receiving telescope has a 61 cm diameter. The back scattered return is focused on a 1 mm fiber optic cable and guided to the detector box on the back of the control unit. We measure the return of the atmospheric rotational Raman scatter at 530 nm and 528 nm and the vibrational Raman scatter from water vapor at 660 nm and 295 nm respectively, from nitrogen at 607 nm and 284 nm respectively and from oxygen at 277 nm. All seven wavelengths are detected by photo multiplier tubes (PMT) and sampled with a 100 MHZ counting device which integrates a profile each minute. The data are collected with 75 m height resolution from the surface up to 12 km. An X-band radar with a 6° cone angle provides an automatic shutdown to prevent a possible illumination of an air plane with the beam.

3 PURE ROTATIONAL RAMAN TEMPERATURE MEASUREMENTS

The pure rotational Raman temperature measurement technique makes use of the temperature dependence of the rotational Raman spectrum of N_2 and O_2. In Figure 1 we show the pure rotational Raman spectrum of N_2 and O_2 scattered from the second harmonic of a Nd:YAG laser.[7] At atmospheric temperatures, the rotational energy states of the molecules are populated to a high degree and the distribution of the spectrum in anti-Stoke's and Stoke's wings represent the thermal equilibrium distribution of the states. In the anti-Stoke's region the scattered photons have a higher energy than the incident photons. We use the anti-Stokes spectral region in order to avoid possible contamination from fluorescence.[6] We measure the return around 530 nm and 528 nm with two narrow band filters in order to determine the temperature. The lidar ratio R of these returns can be expressed as a function of the temperature T as,

$$R(T) = \frac{\sum_S \sum_J N_s \times A_S(J,T) \times f_{530,S}(J)}{\sum_S \sum_J N_s \times A_S(J,T) \times f_{528,S}(J)} = \frac{C_{530}}{C_{528}}, \quad (1)$$

where S is the summation over the molecular species, e.g. N_2 and O_2, and J is the summation over the quantum numbers of the rotational states. N_S is the fraction of the species in the atmosphere, $A_S(J,T)$ is the thermal population distribution of the rotational states and $f_{530,S}(J)$, $f_{528,S}(J)$ are the filter transmission functions of the two channels at the corresponding wavelengths. The ratio is only dependent on the molecular density ratio, which is constant for N_2 and O_2, and the temperature. With increasing temperature higher rotational states are populated. As a result the spectrum

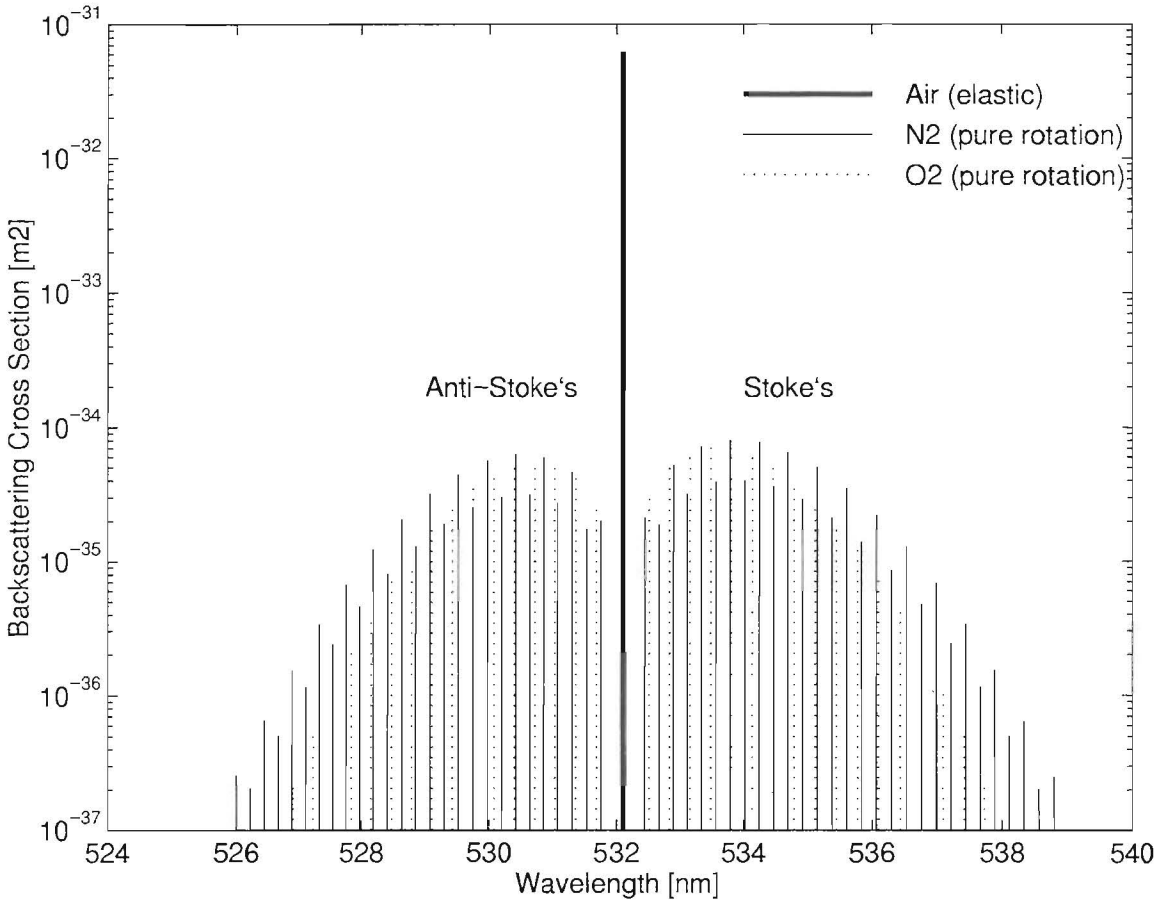

Figure 1: Calculated quantum rotational line intensities for nitrogen and oxygen at a temperature of 310 K, along with the elastic backscatter cross section of air. The rotational intensities include the species' fraction of air. The calculations are made for the second harmonic of the Nd:YAG laser at 532.1 nm.

becomes broader, intensities of the lines further away from the 532.1 nm line increase and the line intensities closer to 532.1 nm decrease. Consequently the count rates in the 528 nm channel increase with temperature while the count rates of the 530 nm channel decrease at a given range bin. The question of weather the rotational Raman return of H_2O has an impact on the measured ratio has been investigated.[7] This systematic error was estimated to be smaller than 0.2 K. The integral intensity of the rotational Raman bands is about two orders of magnitude smaller than the molecular scatter at the fundamental wavelength. The bands are spectrally very close together so that the measured ratio is hardly affected by differential extinction. This technique, is thus particularly well suited to measure temperature in the troposphere.

4 DATA ANALYSIS

The lidar equation describes the different factors that have an influence on the intensity of the

return of a laser beam as a function of range and wavelength.[8] It is evident that taking the ratio of two wavelengths eliminates all range dependent factors. Wavelength dependent factors, such as detector sensitivity, can be expressed as a calibration factor, however, wavelength and range dependent factors, such as transmission must be corrected. However, in case of the rotational Raman temperature technique the two observed spectral intervals are very close together, so that essentially no correction is needed.

First, the count rates of the different wavelengths are calculated by subtracting the measured background of each channel from the signal. Then the count rates are corrected for saturation of the PMT's due to single overlap of consecutive pulses.[9] Although the relation between the temperature and the measured ratio is given from first principles in Equation 1, it would not be efficient to solve this equation and to determine the necessary instrumental parameters in order to determine the temperature. We calibrate our lidar by comparing the lidar ratio with a simultaneous temperature profile taken by balloon . In Figure 2 we present such a comparison for three launches of Vaisala RS 80-15 sondes. The lidar data is integrated for 30 minutes starting at the time of the balloon

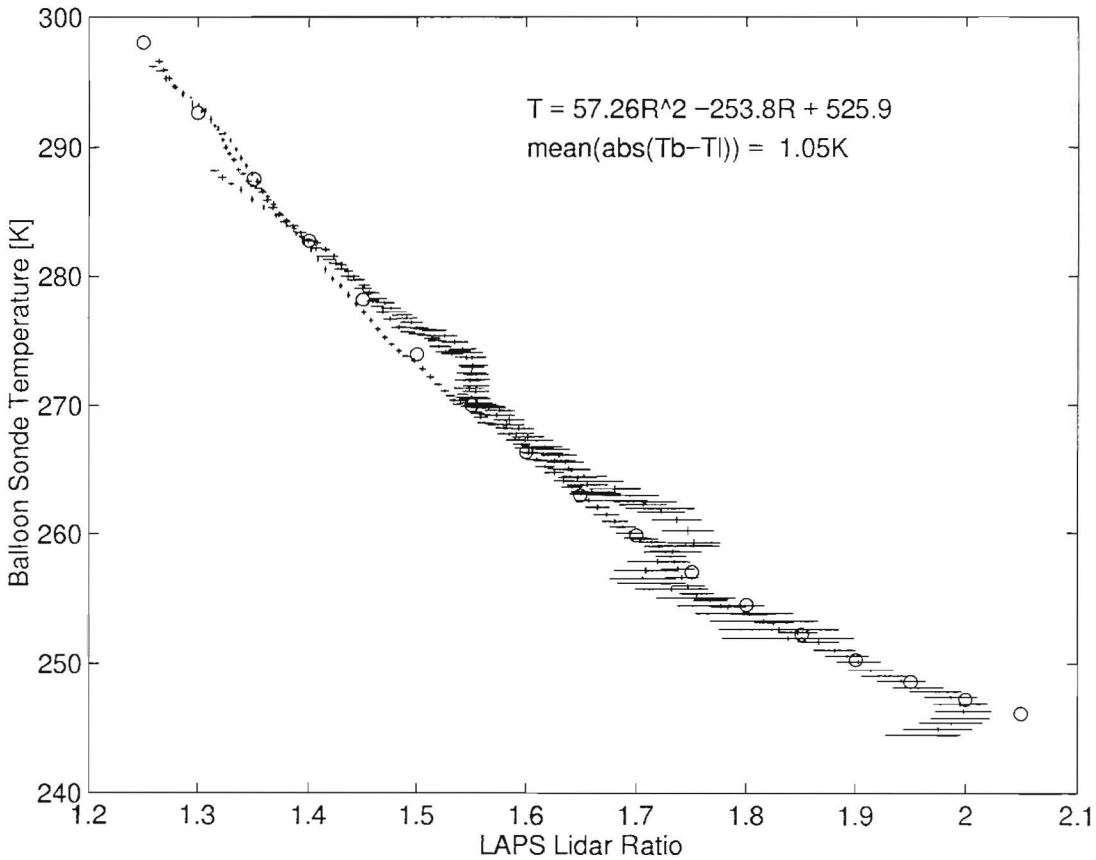

Figure 2: Calibration data for the rotational Raman temperature technique. The plot shows the comparison between balloon temperature profiles and LAPS lidar ratio profiles for the evenings of the 30 May, 6 June and 10 June 1996 measured in State College, PA. Each lidar ratio value is plotted against the corresponding balloon temperature. The bars indicate the 1σ error of the measurement.

launch. At each 75 m lidar range bin the lidar ratio, with its 1σ error bar, is plotted against the mean balloon temperature and its variation in the same bin. The lidar data has been filtered in order to distinguish the three data sets. The filtering process has only a minor influence on the further analysis. For the calibration, we expand Equation 1 in a second order Taylor series,

$$T(R) = a \times R^2 + b \times R + c. \tag{2}$$

This equation is fitted, with a least square method, to the data shown in Figure 2 taking both statistical error of the lidar ratio and temperature variation over a range bin into account. To calculate the calibration constants we take data from several nights. This provides a statistical averaging of the atmospheric variability since at higher altitudes, the balloon measures at a different place, where the temperature might differ from the vertical lidar profile (see section 5).

A calculation of measurement error is obtained by treating the integrated counts as Gaussian distributed variables, although they are given as a difference of two Poisson distributed variables. By only considering points with an error of the lidar ratio smaller than 10 to 20 %, this simplification leads to valid estimates of the measurement error.

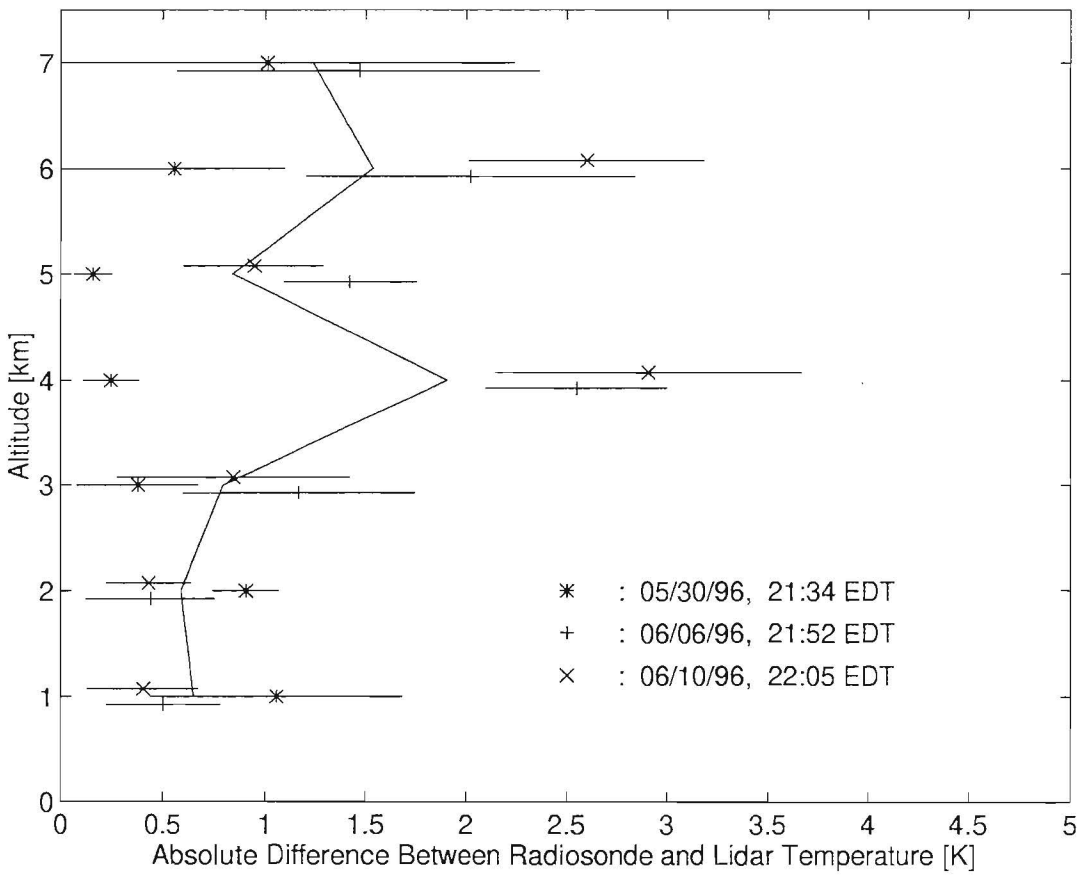

Figure 3: For data already shown in Figure 2, the absolute difference between the sonde temperature and the lidar temperature is given as a function of altitude. The lidar temperature is calculated with the coefficients indicated in Figure 2. The points show the difference for each of the days with the statistical variation over 1 km, the line is the average of all the three days.

5 MEASUREMENTS

Figure 3 shows the absolute difference between the radiosonde temperature and the lidar temperature as a function of altitude. We calculated the lidar temperature with the calibration coefficient curve (circle points, which correspond to the given equation) shown in Figure 2. The points indicate the difference for each of the runs (mean value and standard deviation over 1 km), the solid line shows the average for the three days. The difference between the two techniques is smaller than one degree Kelvin below 3 km altitude. Up to 7 km the difference is well below 2 K. Above 3 km there is also a big variation from day to day as well at different altitudes. This indicates that at higher altitudes not only the lower signal to noise of the lidar causes the larger difference between the two methods, but also at higher altitude the balloon sonde makes its measurement at a different place than the lidar. We have observed horizontal displacements of more than 15 km at 5 km altitude. It is possible to observe differences of temperature in the order of one to two degrees

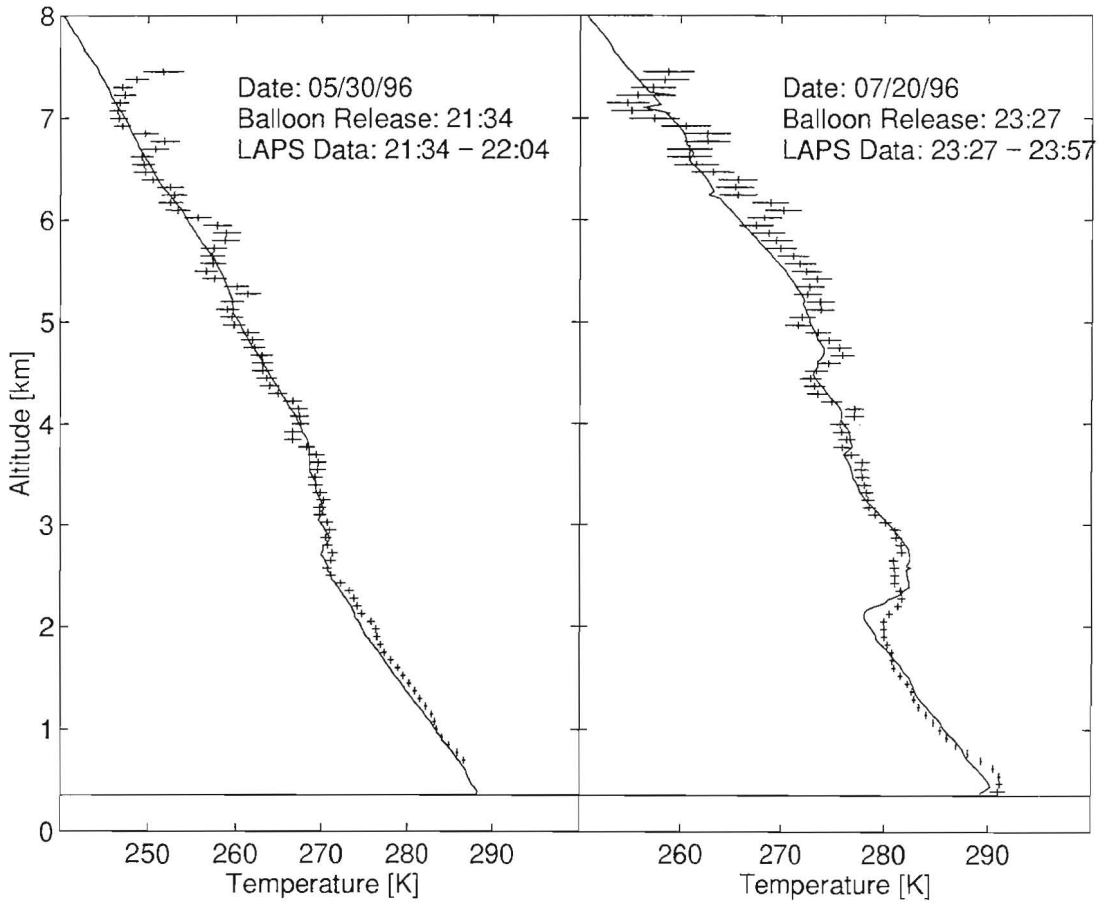

Figure 4: Two comparisons of radiosonde temperature profiles (solid line) with lidar profiles. The horizontal bar indicates the 1σ error bar of the lidar measurement. The lidar data is filtered with a Hanning filter. Both examples were measured at State College, PA. The integration for 30 minutes of the lidar profile starts at the balloon launch.

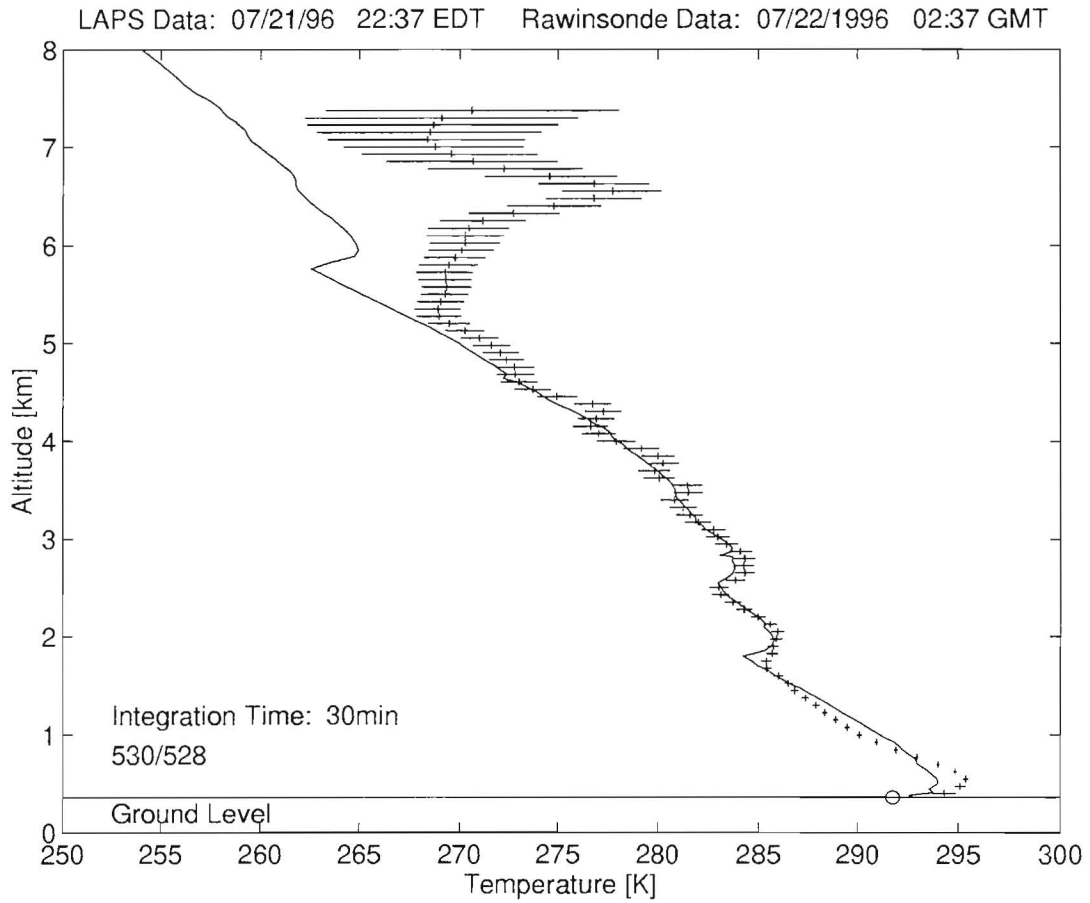

Figure 5: Comparison of a radiosonde temperature profile (solid line) with a lidar profile measured in State College, PA on 22 July 1996. The horizontal bar indicate the 1σ error bar of the lidar measurement. The lidar data is filtered with a Hanning filter. Above 5.3 km the two profiles show a different shape.

Kelvin over this horizontal distance. As mentioned earlier the numbers above are calculated with the average calibration constants for the three days. If we calculate the constants for every night and determine the difference between balloon and lidar, the values become about 15 % smaller. This indicates that we are maintaining stable operating conditions for the lidar over a longer period of time.

In Figures 4 and 5 three comparisons between radiosonde and lidar temperature profiles are presented. All the measurements were taken in State College, PA, and the lidar data have been smoothed with a Hanning filter. In Figure 4 both techniques produce similar profiles. Above 4 km the lidar temperature profile shows a little more wave structure than the radiosonde. The statistical error for a 30 minute profile is on the order or smaller than 1 K up to a range of 5 km. In Figure 5, the two temperature profiles agrees within their error bars up to 5.3 km. Above 5.3 km, the lidar shows a strong departure in the temperature profile compared to the radiosonde. The analysis of the water vapor channels showed that during the same time interval ($\approx$22:45 – 23:15) an increase of the water vapor mixing ratio occured between 5.5 and 6.5 km. The difference is due to the advection of

the atmosphere past the lacation. The air mass which is carring the balloon is significantly different from that present directly above the lidar site.

6 SUMMARY

We have demonstrated the capability of LAPS to measure temperature in the lower half of the troposphere. With the rotational Raman technique we obtain profiles with errors on the order or smaller than 1 K up to 5 km altitude with 30 minutes lidar signal integration. Comparisons with radiosonde temperature profiles show a good agreement in most the cases. The permanent sampling volume of the lidar is an advantage for the recording and the understanding of certain meteorological conditions.

7 ACKNWLEDGEMENTS

Special appreciation for the support of this work goes to NCCOSC NRaD and SPAWAR PMW–185. The work of F. Balsiger was partly sponsored by the Swiss National Science Foundation. We thank E. F. Boone, M. J. Bregar, D. L. McDowell, G. Pancoast, T. M. Petach, D. B. Lysak and R. W. Smith for their efforts in building the system and their support in obtaining the data.

8 REFERENCES

1. C. R. Philbrick, "Raman lidar measurements of atmospheric properties," Atmospheric propagation and remote sensing III, SPIE Vol **2222**, 922–931, 1994.

2. Y.-C. Rau, "Multi-wavelength Raman-Rayleigh lidar for atmospheric remote sensing," PhD dissertation, Penn State University, 1994.

3. J. Cooney, "Measurement of atmospheric temperature profiles using the Raman component of laser backscatter," *J. Appl. Meteo.* 11, 108-112, 1972.

4. Yu. F. Arshinov, S. M. Bobrovnikov, V. E. Zuev and V. M. Mitev, "Atmospheric temperature measurements using a pure rotational Raman lidar," *Appl. Optics,* **22**, 2984-2990, 1983.

5. A. Hauchecorne, M. L. Chanin, P. Keckhut, and D. Nedeljkovic, "Lidar monitoring of the temperature in the middle and lower atmosphere," *Appl. Phys.* B55, 29-34, 1992.

6. D. Nedeljkovic, A. Hauchecorne and M. L. Chanin, "Rotational Raman lidar to measure the temperature from the ground to 30 km," *IEEE Trans. Geos. Remote Sens.* 31, 90-101, 1993.

7. P. A. T. Haris, "Pure rotational Raman lidar for temperature measurements in the lower troposphere," PhD Dissertation, Department of Electrical Engineering, The Pennsylvania State University, 1995.

8. R. M. Measures, *Laser Remote Sensing,* Chapter 7, Krieger Publishing Company, Malabar FL, 1992.

9. D. P. Donovan, J. A. Whiteway, and A. I. Carswell, "Correction for nonlinear photon–counting effects in lidar systems," *Applied Optics*, Vol. 32, No 33, 6742–6753, 1993.